Kel1p Mediates Yeast Cell Fusion Through a Fus2p- and Cdc42p-Dependent Mechanism

Jean A. Smith and Mark D. Rose[1]
Department of Molecular Biology, Princeton University, New Jersey 08544
ORCID ID: 0000-0003-1112-4765 (M.D.R.)

ABSTRACT Cell fusion is ubiquitous among eukaryotes. Although little is known about the molecular mechanism, several proteins required for cell fusion in the yeast *Saccharomyces cerevisiae* have been identified. Fus2p, a key regulator of cell fusion, localizes to the shmoo tip in a highly regulated manner. C-terminal truncations of Fus2p cause mislocalization and fusion defects, which are suppressed by overexpression of Kel1p, a kelch-domain protein of unknown function previously implicated in cell fusion. We hypothesize that Fus2p mislocalization is caused by auto-inhibition, which is alleviated by Kel1p overexpression. Previous work showed that Fus2p localization is mediated by both Fus1p- and actin-dependent pathways. We show that the C-terminal mutations mainly affect the actin-dependent pathway. Suppression of the Fus2p localization defect by Kel1p is dependent upon Fus1p, showing that suppression does not bypass the normal pathway. Kel1p and a homolog, Kel2p, are required for efficient Fus2p localization, acting through the actin-dependent pathway. Although Kel1p overexpression can weakly suppress the mating defect of a *FUS2* deletion, the magnitude of suppression is allele specific. Therefore, Kel1p augments, but does not bypass, Fus2p function. Fus2p mediates cell fusion by binding activated Cdc42p. Although Kel1p overexpression suppresses a Cdc42p mutant that is defective for Fus2p binding, cell fusion remains dependent upon Fus2p. These data suggest that Fus2p, Cdc42p, and Kel1p form a ternary complex, which is stabilized by Kel1p. Supporting this hypothesis, Kel1p interacts with two domains of Fus2p, partially dependent on Cdc42p. We conclude that Kel1p enhances the activity of Fus2p/Cdc42p in cell fusion.

KEYWORDS kelch protein; conjugation; yeast mating

CELL fusion is an essential and ubiquitous process in eukaryotic organisms, with many examples of cell fusion events throughout embryogenesis and development. In mammals, these include sperm–egg fusion during fertilization (Wassarman and Litscher 2008), placental trophoblast fusion during pregnancy (Huppertz and Borges 2008), and the fusion of myoblasts to form myofibers during skeletal muscle development (Kim *et al.* 2015). Blocks in placental trophoblast fusion have been correlated with preeclampsia during pregnancy (Gauster *et al.* 2009). Despite the importance of these events, little is known about the molecular mechanisms that control cell fusion.

During mating of the budding yeast, *Saccharomyces cerevisiae*, two haploid cells of opposite mating types fuse to form a diploid zygote, making this organism an excellent model to study cell fusion (Ydenberg and Rose 2008; Merlini *et al.* 2013). The yeast mating pathway begins with pheromone recognition and subsequent activation of a well-characterized kinase cascade. The results of the cascade are the activation of mating-specific genes, cell-cycle arrest, and polarized growth along the pheromone gradient toward the mating partner. The formation of the mating projection causes the cell to become pear shaped, a form commonly called a "shmoo," and the tip comes into contact with its partner cell, forming the zone of cell fusion. As such, the shmoo tip constitutes a localization hub for many proteins necessary for cell fusion (Ydenberg and Rose 2008).

Genetic studies have identified four shmoo-tip-localized proteins (Fus1p, Fus2p, Rvs161p, and Prm1p) likely to play direct roles in the fusion pathway. *FUS1*, *FUS2*, and *PRM1* are all pheromone-induced genes and are required in at least one of two mating cells to produce a diploid. Rvs161p is a BAR domain protein related to amphiphysin that plays a role in endocytosis in mitotic cells by stabilizing curved membranes (Crouzet *et al.* 1991; Friesen *et al.* 2006). Therefore, *RVS161*

doi: 10.1534/genetics.115.185207
Manuscript received November 23, 2015; accepted for publication February 5, 2016; published Early Online February 8, 2016.
[1]Corresponding author: Department of Molecular Biology, Princeton University, Princeton, NJ 08544-1014. E-mail: mdrose@princeton.edu

is expressed in mitotic cells, but strongly induced by pheromone (Brizzio *et al.* 1998). Fus2p and Rvs161p form a complex, which is transported to the shmoo tip in an actin- and Myo2p-dependent manner (Brizzio *et al.* 1998; Paterson *et al.* 2008; Sheltzer and Rose 2009), and anchored at the cortex in a mechanism requiring both actin and Fus1p (Paterson *et al.* 2008). Mutations in *FUS1*, *FUS2*, and *RVS161* block the removal of cell wall material between two mating cells (Trueheart *et al.* 1987; Trueheart and Fink 1989; Brizzio *et al.* 1998). Deletion of both *FUS1* and *FUS2* causes a more severe mating phenotype than either single deletion alone, suggesting that *FUS1* and *FUS2* have some nonoverlapping functions (Trueheart *et al.* 1987; Gammie *et al.* 1998). Prm1p acts after cell wall removal, to facilitate plasma membrane fusion (Heiman and Walter 2000).

One of the key morphological events observed before fusion occurs is the clustering of vesicles at the center of the zone of cell fusion. These vesicles are smaller than mitotic vesicles, suggesting that they are mating specific (Baba *et al.* 1989). The vesicles remain closely associated with the residual cell wall after fusion (Gammie *et al.* 1998). Cells lacking *FUS1* fail to localize the vesicles to the center of the zone of cell fusion, while *fus2* and *rvs161* mutants localize the vesicles normally, suggesting that the Fus2p–Rvs161p complex acts after vesicle clustering, and thus later than Fus1p (Trueheart *et al.* 1987; Gammie *et al.* 1998). Fus2p is thought to regulate the fusion of the vesicles to the plasma membrane, releasing hydrolases that break down the cell wall between mating cells (Gammie *et al.* 1998; Paterson *et al.* 2008).

Fus2p contains a Dbl-homology domain, similar to Rho-type GTP exchange factors (GEFs). The Dbl-homology domain is required for Fus2p function, suggesting that Fus2p acts with a Rho-GTPase. In support of this hypothesis, Fus2p binds to Cdc42p, and alleles of *cdc42* defective for Fus2p binding exhibit a cell fusion defect (Ydenberg *et al.* 2012). Cdc42p is a Rho-like GTPase that plays numerous roles in growth and morphogenesis (Richman *et al.* 1999; Johnson 1999; Kozminski *et al.* 2000; Adamo *et al.* 2001). Fus2p preferentially interacts with GTP-bound Cdc42p, suggesting that it is an effector or recruiter of activated Cdc42p, rather than a GEF (Nelson *et al.* 2004; Ydenberg *et al.* 2012).

Through deletion analysis, we have shown that the last eight amino acids of Fus2p are required for its localization to the shmoo tip (Stein *et al.* 2015). Saturation mutagenesis identified several point mutations in this region of the protein that cause severe mating and localization defects comparable to the truncation. The C-terminal mutant proteins are stable and bind both Rvs161p and Cdc42p, so the localization and mating phenotypes are not due to lack of interaction with the known binding partners (Ydenberg *et al.* 2012).

Here, we identify *KEL1* as a high-copy suppressor of the mating phenotype of both the C-terminal truncation (*fus2-670*$_{UAG}$) and the point mutant (*fus2-L674A*). *KEL1* encodes a conserved kelch-domain protein. Kelch domains are typically found in 4–7 repeats and form β-propeller structures. Proteins containing kelch domains have a diverse array of activities in multiple cellular compartments. The kelch domain, however, is thought to assist protein–protein interactions, and many kelch domain-containing proteins are involved in regulating or binding to actin (Adams *et al.* 2000). *KEL1* was previously discovered as a high-copy suppressor of a mating defect caused by an overactive allele of protein kinase C (Philips and Herskowitz 1998), which activates the cell wall integrity pathway in yeast (Davenport *et al.* 1995). The cell fusion phenotype seen with this mutant led to the hypothesis that the cell wall integrity pathway negatively regulates fusion, possibly in response to osmolarity (Philips and Herskowitz 1997). A paralog of *KEL1*, *KEL2*, was also identified and shown to be able to suppress overactive Pkc1p to a lesser extent. Genetic analysis led to the hypothesis that *KEL1* and *KEL2* may play roles in activation of cell fusion (Philips and Herskowitz 1998); however, their specific functions were not investigated further. We have found that *KEL1* is required for efficient cell fusion as well as Fus2p localization, and that Kel1p and Fus2p interact in mating cells.

Materials and Methods

General yeast techniques

Yeast media, general methods, and transformations were performed as described previously (Amberg *et al.* 2005) with minor modifications. Strains and plasmids are listed in Table 1 and Table 2. All strains and plasmids are available upon request. Deletion strains were created via PCR amplification of selective markers and homologous recombination at the locus of interest. Mutations in pMR6441 and pMR5482 were created via PCR-mediated site-directed mutagenesis. Truncations of Fus2p were made by introducing a stop codon at the residue of interest. Kel1p was tagged with 3× HA at the C terminus via PCR and homologous recombination at the *KEL1* locus.

All strains were grown at 30°. For pheromone induction experiments, early exponential cells growing in selective media were treated for 90 min with synthetic α-factor (Department of Molecular Biology Syn/Seq Facility, Princeton University) added to a final concentration of 10 μg/ml. Strains induced with galactose were grown overnight, diluted, and allowed to grow to early log phase in media containing 2% raffinose. The cells were then treated with 2% galactose concurrently with pheromone induction.

Yeast mating assays

Limited plate mating assays and quantitative filter matings were performed as described previously with minor alterations (Gammie and Rose 2002). Briefly, limited plate mating assays used a lawn of the *MAT*α strain grown on rich media plates and patches of the *MAT***a** strains grown on selective media. The strains were replica plated together onto rich media, allowed to mate for 3 hr at 30°, and then replica plated onto media selective for diploids. Mating efficiency was assessed after 2 days of growth at 30°.

Table 1 Yeast strains

Strain	Genotype	Source
BY4741	*MAT***a** *his3-d1 leu2-d0 ura3-d0 met15-d0*	Brachmann *et al.* (1998)
DDY1300	*MAT***a** *ura3-52 leu2-3112 his3Δ200 lys2-801 CDC42::LEU2*	Kozminski *et al.* (2000)
DDY1354	*MAT***a** *ura3-52 leu2-3112 his3Δ200 lys2-801 cdc42-138::LEU2*	Kozminski *et al.* (2000)
JY428	*MATα fus2-d3 his4-d34 trp1-d1 ura3-52 can^r* G. Fink (Whitehead Institute, Cambridge, MA)	
JY429	*MATα trp1-d1 ura3-52 cyh2 fus1-d1 fus2-d3*	G. Fink (Whitehead Institute, Cambridge, MA)
MY10904	*MAT***a** *fus2::HIS3 RVS161-Flag$_{85}$ ura3Δ0 leu2Δ0 his3Δ1 met15Δ0*	Stein *et al.* (2015)
MY10935	*MAT***a** *fus2::HIS3 fus1::NatMX ura3Δ0 leu2Δ0 his3Δ1 met15Δ0*	
MY13522	*fus2::HIS3 RVS161-Flag$_{85}$ ura3d0 leu2do his3d1 met15d0 kel11::pGal1-KEL1-KanMX*	
MY13675	*MAT***a** *kel1::KanMX his3d1 leu2d0 ura3d0 met15d0*	
MY13764	*MAT***a** *fus2::HIS3 kel1::KanMX his3d1 leu2d0 ura3d0 met15d0*	
MY13916	*MAT***a** *fus2::HIS3 fus1::NatMX kel1::kanMX ura3d0 leu2d0 his3d1 met15d0*	
MY13965	*MAT***a** *fus2::HIS kel2::KanMX his3Δ1 leu2Δ0 ura3Δ0 met15Δ0*	
MY14200	*MAT***a** *fus2::HIS3 kel1::NatMX kel2::KanMX ura3d0 leu2d0 his3d1 met15d0*	
MY14339	*MAT***a** *fus2::HIS3 kel1::NatMX kel2::KanMX fus1::URA3 ura3d0 leu2d0 his3d1 met15d0*	
MY14545	*MAT***a** *fus2::HIS3 fus1::Nat kel2::KanMX ura3d0 leu2d0 his3d1 met15d0*	
MY15063	*MAT***a** *fus2::his3 KEL1-3xHA-KanMX ura3d0 leu2d0 his3d1 met15d0*	
MY15471	*MAT***a** *CDC42-LEU2 fus2::NatMX lys2-801 ura3-52 leu2-3,112 his3-d200*	
MY15472	*MAT***a** *CDC42-LEU2 kel1::KanMX lys2-801 ura3-52 leu2-3,112 his3-d200*	
MY15473	*MAT***a** *cdc42-138-LEU2 lys2-801 ura3-52 leu2-3,112 his3-d200*	
MY15474	*MAT***a** *cdc42-138-LEU2 fus2::NatMX lys2-801 ura3-52 leu2-3,112 his3-d200*	
MY15475	*MAT***a** *cdc42-138::LEU2 kel1::KanMX lys2-801 ura3-52 leu2-3,112 his3-d200*	
MY7926	*MAT***a** *CDC42-LEU2 lys2-801 ura3-52 leu2-3,112 his3-d200*	Ydenberg *et al.* (2012)
MY9181	*MAT***a** *fus2::HIS his3-d1 leu2-d0 ura3-d0 met15-d0*	Paterson *et al.* (2008)

Quantitative filter matings were performed by mixing early exponential *MAT***a** cells with *MAT*α cells at a 1:4 ratio of optical density units to reach a total of $\sim 1 \times 10^7$ cells/ml. This ratio was determined to be optimal for mating efficiency of the *MAT***a** cells, while showing the lowest variance. The cells were mixed together, concentrated on 25 mm 0.45-μm nitrocellulose filter disks (Millipore), and incubated on rich media plates for 2.5–5 hr at 30°. Mating mixtures were resuspended in 1 ml dH_2O, serially diluted, and sonicated in a bath sonicator at low power for 3 min. The dilutions were plated on selective media for the *MAT***a**, *MAT*α, and diploid strains, and then grown at 30° for 2 days. The frequency of diploid formation was normalized to the number of cells containing the plasmid. Two-tailed, paired *t*-tests were used to obtain *P*-values for data from quantitative filter matings. In figures reporting quantitative mating frequencies, the error bars show the standard error of the mean, from a minimum of three experiments.

High-copy suppression of Fus2p C-terminal mutations

A YEp13-based yeast genomic DNA library (Broach *et al.* 1979) was transformed into *MAT***a** *fus2*Δ strain containing a centromere-based plasmid with *fus2-L674A* (MY11879). Approximately 20,000 transformants were mated to a *MAT*α *fus1*Δ*fus2*Δ lawn (JY429) as described above. Plasmids showing suppression were recovered from the cells (Amberg *et al.* 2005), transformed into MY11879, and retested. DNA sequencing was used to identify the genes carried on the suppressing plasmids.

Microscopy

For imaging of pheromone-induced cells with fluorescent proteins, cells were induced as described above, fixed for 10 min with 2% formaldehyde at 30°, and then imaged. All images were acquired at 23° using a deconvolution microscopy system (DeltaVision; Applied Precision) equipped with an inverted microscope (TE200; Nikon) and a ×100 objective with numerical aperture of 1.4. Chi square statistical tests were used to obtain *P*-values for microscopy data.

Microscopic assays of FM4-64 stained mating mixtures were performed as described previously (Grote 2008). Briefly, mating mixtures were prepared as described above, but resuspended in 1 ml of TAF (20 mM Tris-HCl pH 7.4, 20 mM NaN_3, 20 mM NaF) buffer and kept on ice. FM4-64 (Molecular Probes/Invitrogen) was added to mating mixtures to a final concentration of 4 μM and stained zygotes were imaged as above. In all figures reporting quantitative scoring of Fus2p localization in shmoos or cell fusion in zygotes, the error bars show the standard error of the sample proportion, using aggregated data from a minimum of three independent experiments.

Table 2 Plasmids

Strain	Genotype	Reference
pMR5469	*pGAL1-FUS2-GFP$_{104}$ URA3 CEN3 amp^R*	Paterson *et al.* (2008)
pMR5482	*FUS2-GFP$_{104}$ URA3 CEN3 amp^R*	Paterson *et al.* (2008)
pMR5774	*pGAL1-FUS2$^{1-104}$-GFP URA3 CEN3 amp^R*	Ydenberg and Rose (2009)
pMR5784	*pGAL1-FUS2$^{105-677}$-GFP$_{104}$ URA3 CEN3 amp^R*	Stein *et al.* (2015)
pMR5883	*pGAL1-FUS2$^{\Delta 105-415}$-GFP$_{104}$ URA3 CEN3 amp^R*	
pMR5884	*pGAL1-FUS2$^{415-677}$-GFP$_{104}$ URA3 CEN3 amp^R*	Stein *et al.* (2015)
pMR5886	*pGAL1-FUS2$^{1-580}$-GFP$_{104}$ URA3 CEN3 amp^R*	Stein *et al.* (2015)
pMR6441	*KEL1 REC104 LEU2 2μ amp^R*	
pMR6499	*pGAL1-FUS2-GFP$_{104}$-M650$_{UAG}$ URA3 CEN3 amp^R*	Stein *et al.* (2015)
pMR6501	*FUS2-GFP$_{104}$-L674A URA3 CEN3 amp^R*	Stein *et al.* (2015)
pMR6730	*KEL1-K102$_{UAA}$ REC104 LEU2 2μ amp^R*	This study
pMR6731	*KEL1 REC104-I3$_{UAA}$ LEU2 2μ amp^R*	This study
pMR6775	*FUS2-GFP$_{104}$-670$_{UAG}$ URA3 CEN3 amp^R*	Stein *et al.* (2015)
pMR6806	*KEL1 HIS3 2μ amp^R*	
pMR6824	*FUS2-GFP$_{104}$-D639AURA3 CEN3 amp^R*	
pMR6826	*FUS2-GFP$_{104}$-L641AURA3 CEN3 amp^R*	
pMR6851	*FUS2-GFP$_{104}$-W659AURA3 CEN3 amp^R*	
pMR6852	*FUS2-GFP$_{104}$-660$_{UGA}$ URA3 CEN3 amp^R*	
pMR6853	*FUS2-GFP$_{104}$-650$_{UAG}$ URA3 CEN3 amp^R*	
pMR6854	*FUS2-GFP$_{104}$-640$_{UGA}$ URA3 CEN3 amp^R*	
pMR6953	*KEL1-3xHA LEU2 2μ amp^R*	
pMR7008	*FUS2-GFP$_{104}$-416$_{UAA}$ URA3 CEN3 amp^R*	
pMR7026	*KEL1-3xHA HIS3 2μ amp^R*	
pRS416	*URA3 CEN3 ARS1 amp^R*	Sikorski and Hieter (1989)
pRS423	*HIS3 2μ amp^R*	Sikorski and Hieter (1989)
pRS425	*LEU2 2μ amp^R*	Sikorski and Hieter (1989)
YEp13	*LEU2 2μ amp^R*	Broach *et al.* (1979)

Latrunculin A treatment

Pheromone-induced cells were prepared as described above, and then concentrated 5× in selective media with α-factor via filtration to preserve actin morphology. Next, 50 μl of cells was incubated for 5 min at 30° with either 2% DMSO (mock) or latrunculin A (Invitrogen) at a final concentration of 200 μM in DMSO. Samples were put on ice to be imaged as above. To visualize actin, a subset of mock- or LatA-treated cells was fixed in 3.7% formaldehyde for 10 min at 30°, washed with PBS, resuspended in 50 μl PBS, and incubated with 25 μl Texas Red-X Phalloidin (0.2 units/μl; Invitrogen) for 1 hr at room temperature in the dark. The cells were washed in PBS and examined by fluorescence microscopy as above.

Co-immunoprecipitations and Western blotting

Cell extracts were prepared from 100 ml of pheromone-induced yeast cultures which had been frozen in liquid nitrogen and stored at −80°. Cells were lysed using acid-washed glass beads (BioSpec) in lysis buffer containing 50 mM Tris-HCl, pH 7.4, 150 mM NaCl, 10% glycerol, 10 mM EDTA, 100 mM β-glycerophosphate, 50 mM NaF, 5 mM $NaVO_3$, 1% Triton X-100, 5 mM PMSF, and complete EDTA-free protease inhibitor cocktail (Roche). The extract was removed from the glass beads and clarified by centrifugation at 11,000 rpm in a microcentrifuge for 10 min at 4°. Lysates were incubated with anti-HA magnetic beads (Thermo Scientific) for 1 hr at room temperature with rotation, washed two times with PBS, and boiled for 5 min in sample buffer as described previously (Ohashi *et al.* 1982) before loading onto 10% SDS-PAGE gels. After separation via SDS-PAGE, proteins were transferred to a nitrocellulose membrane. GFP-tagged Fus2p was detected using mouse anti-GFP (Clontech, 1:1000). HA-tagged Kel1p was detected using mouse anti-HA (Santa Cruz, 1:1000). Two-tailed, paired *t*-tests were used to obtain *P*-values for data from immunoprecipitations.

Data availability

All strains and plasmids are available upon request. Strains and plasmids used in this study are presented in Table 1 and Table 2.

Results

Isolation of high-copy suppressors of fus2-L674A

The localization of Fus2p at the cell cortex during mating is controlled by several different protein domains (Figure 1A). The N-terminal domain (NTD) controls trafficking between the nucleus and cytoplasm (Ydenberg and Rose 2009; Kim and Rose 2012). Fus2p forms a heterodimer with an amphiphysin, Rvs161p, which is required for stability and localization to the shmoo tip (Brizzio *et al.* 1998; Paterson *et al.* 2008). Fus2p also interacts with GTP-bound Cdc42p (Nelson *et al.* 2004; Ydenberg *et al.* 2012), which is required for cell fusion, but not for Fus2p localization (Ydenberg *et al.* 2012). Recently, it was discovered that truncation of the last eight

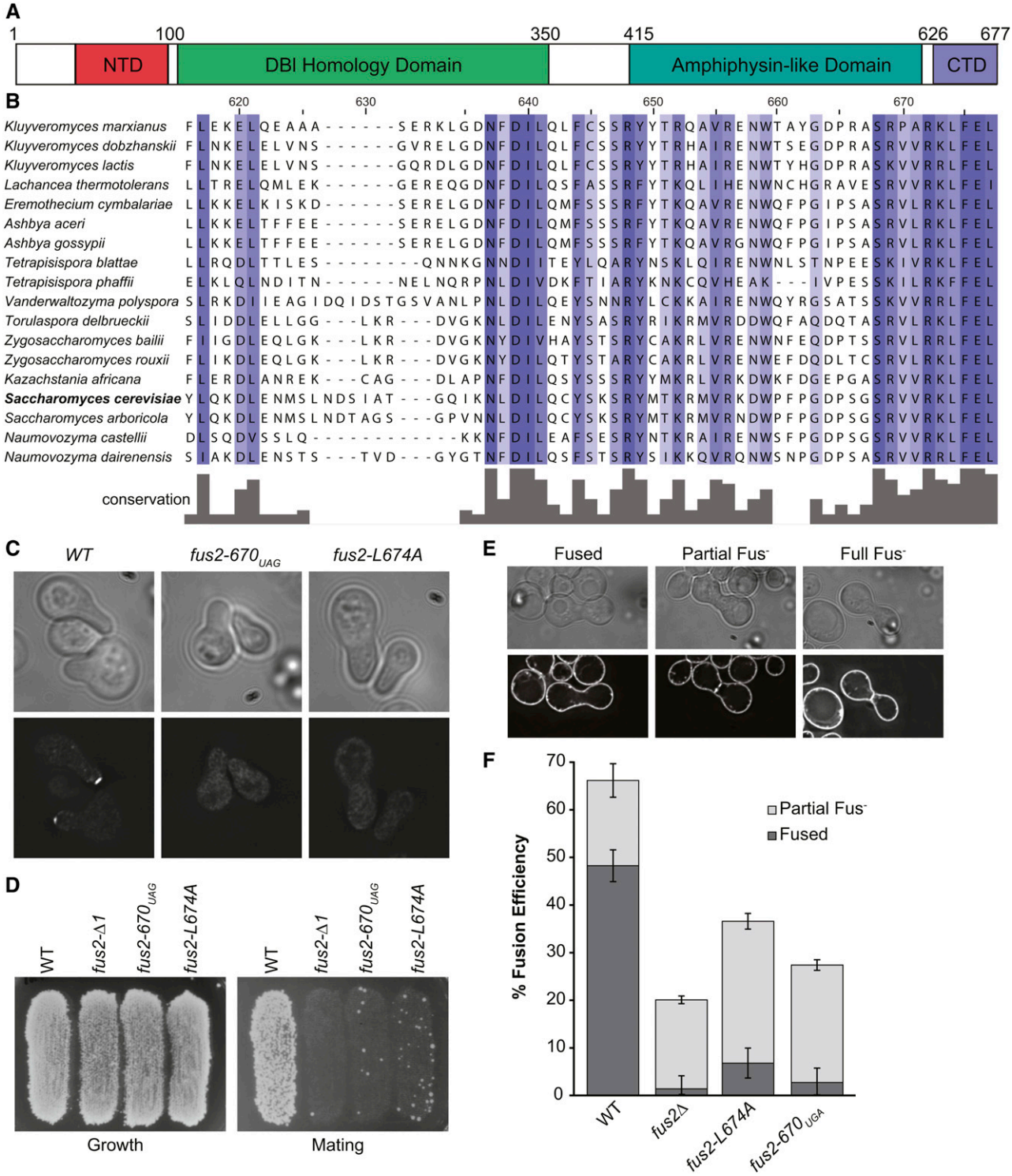

Figure 1 Fus2p C-terminal mutants have localization and mating defects. (A) Conservation of the C terminus of Fus2p. (B) Map of Fus2p primary structure with known domains labeled. (C) Fus2p C-terminal mutants have localization defects. *fus2*Δ cells (MY10904) were transformed with either WT *FUS2* (pMR5482), *fus2-670*$_{UAG}$ (pMR6775), or *fus2-L674A* (pMR6501) all tagged internally with GFP and then imaged after incubation with pheromone for 1.5 hr. (D) Fus2p C-terminal mutants have defects in diploid formation. MY10904 was transformed with plasmids containing either wild-type *FUS2* (pMR5482), *fus2-670*$_{UAG}$ (pMR6775), *fus2-L674A* (pMR6501), or an empty vector (pRS416). The subsequent strains were mated to a *fus1*Δ*fus2*Δ (JY429) for 3 hr at 30°. (E and F) Diploid formation defects correspond to cell fusion defects. The same strains as in D were mated for 3 hr at 30° against *fus2*Δ (JY428), resuspended in TAF buffer, and stained with FM4-64 to stain the plasma membrane. (D) Examples of fusion defective zygotes. (E) Percentage of fully fused and partially fused zygotes observed for each genotype. $n \geq 200$ zygotes imaged in three independent experiments.

amino acids of *FUS2* (*fus2-670$_{UAG}$*) results in diffuse localization of the protein throughout the cell (Stein *et al.* 2015 and Figure 1C). The truncation does not interfere with Rvs161p binding (Stein *et al.* 2015) or Cdc42p binding (Ydenberg *et al.* 2012), indicating that the C-terminal domain (CTD) contains sequences required for cortical localization.

Interestingly, the C terminus of Fus2p is one of the most conserved regions of the protein (Figure 1B); the ten C-terminal residues are almost invariant throughout the family *Saccharomycetaceae*. Each of the C-terminal eight residues was mutated to alanine, and their effects were analyzed. Two point mutations, *fus2-L674A* and *fus2-F675A*, caused severe localization and mating defects, similar to the truncation (Figure 1, C and D and Stein *et al.* 2015). Note that, because the *fus2*Δ mating defect is bilateral, all matings were performed against a *fus2*Δ partner. In most experiments, a *fus1*Δ*fus2*Δ partner was used because a *FUS1* deletion exacerbates the *fus2*Δ mating defect, allowing a more sensitive assay of the mating phenotype.

To determine the cause of the mating defect, *fus2-670$_{UAG}$* and *fus2-L674A* strains were analyzed for their ability to fuse with a *fus2*Δ strain. Zygotes stained with the fluorescent lipid-specific dye FM4-64 showed that both mutants have severe defects in cell fusion (Figure 1, E and F). We conclude that the C-terminal eight residues of Fus2p comprise part of a localization signal required for Fus2p's localization and function.

We reasoned that the point mutations might weaken the interaction of Fus2p with a cortical protein required for its localization to the shmoo tip. To identify potential interacting proteins, we performed a high-copy suppressor screen of the *fus2-L674A* or *fus2-F675A* mating defect using a yeast genomic library (YEp13) (Broach *et al.* 1979). Approximately 20,000 transformants were screened for increased mating ability with a *fus1*Δ*fus2*Δ *MAT*α strain. Four plasmids were identified that reproducibly increased the mating efficiency of the point mutants. One plasmid contained an N-terminal truncation of the open reading frame (ORF) for *MPS1*. *MPS1* is a dual-specificity protein kinase required for spindle pole body duplication and spindle checkpoint function (Winey and Huneycutt 2002). We presume that Mps1p may have additional functions in regulating cell fusion; however, further analysis has not yet been performed on *MPS1* and it will not be described further. The three remaining plasmids contained an identical genomic insert comprising the two genes, *KEL1* and *REC104*. This plasmid, pMR6441, was also capable of suppressing *fus2-670$_{UAG}$* (Figure 2A).

Of the two proteins encoded on the suppressor plasmid, Rec104p functions in meiosis, where it is necessary for the initiation of meiotic recombination (Galbraith and Malone 1993), whereas Kel1p is a kelch domain-containing protein that functions in both mating and mitosis. Kel1p was identified as a suppressor of the cell fusion defect caused by overactive Pkc1p, but its function in mating remained unclear (Philips and Herskowitz 1998). In mating, Kel1p localizes to the shmoo-tip cortex (Philips and Herskowitz 1998). In mitosis, Kel1p localizes to the bud cortex and tethers Lte1p, a member of the mitotic exit network (Höfken and Schiebel 2002; Bertazzi *et al.* 2011). To determine which ORF on the plasmid was responsible for suppression, we created frameshift mutations (*kel1-K102stop* and *rec104-I3stop*) near the

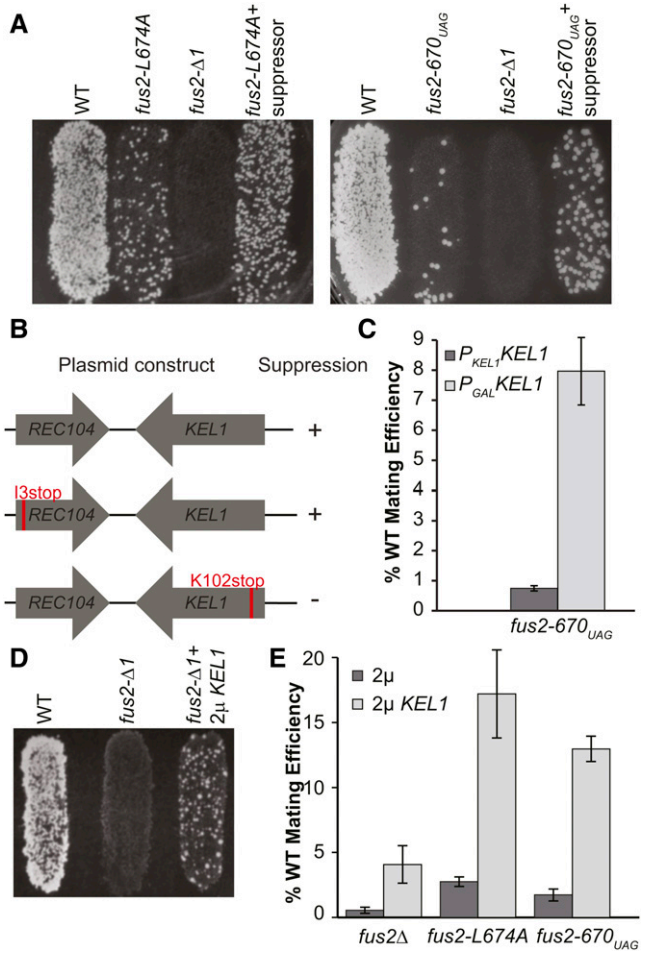

Figure 2 Kel1p overexpression suppresses the mating defect of *fus2* mutations. (A) Suppressor plasmid pMR6441, containing *KEL1* and *REC104* ORFs, partially rescues the mating defect of Fus2p C-terminal mutations. fus2Δ (MY10904) strains already containing a plasmid with either *fus2-L674A* (pMR6501) or *fus2-670$_{UAG}$* (pMR6775) were transformed with either pMR6441 or an empty 2μ plasmid (pRS425). These strains were mated to a *fus1*Δ*fus2*Δ (JY429) for 3 hr at 30°. (B and C) *KEL1* ORF is responsible for the suppression. (B) Two amino acids were inserted near the N termini of either *KEL1* (pMR6730) or *REC104* (pMR6731) in pMR6441 to create a stop codon and frameshift. Suppression was assessed via quantitative filter matings against a *fus1*Δ*fus2*Δ (JY429) for 4 hr at 30°. (C) pMR6775 was transformed into a wild-type *KEL1* strain (MY10904) as well as a strain where *KEL1* was expressed under the control of the *GAL1* promoter integrated at the *KEL1* locus (MY13522). Suppression of *fus2-670$_{UAG}$* was assessed via diploid formation. (D and E) High-copy *KEL1* partially suppresses the mating defect of a complete *fus2* deletion. (D) A *fus2*Δ strain (MY10904) was transformed with pMR6441 or an empty 2μ plasmid (pRS425). These strains were mated to a *fus1*Δ*fus2*Δ (JY429) for 3 hr at 30°. (E) High-copy *KEL1* suppresses C-terminal mutations better than the complete deletion. The same strains as in A and D were mated to a *fus1*Δ*fus2*Δ (JY429) for 4 hr at 30° and suppression was assessed via diploid formation.

N termini of either the *KEL1* or *REC104* ORF on pMR6441. The mutations presumably create null alleles of each gene. When the two mutated plasmids were tested for suppression of the mating defect of *fus2-670*$_{UAG}$, only the plasmid with an intact *KEL1* ORF was functional (Figure 2B). We also expressed *KEL1* under the control of the *GAL1* promoter. When transcription was induced by growth on galactose, the mating defect of *fus2-670*$_{UAG}$ was suppressed (Figure 2C). These results show that *KEL1* is responsible for the suppression of the *fus2* C-terminal mutations.

To determine whether Kel1p suppression requires residual Fus2p function, we analyzed the ability of Kel1p to suppress a complete deletion of *FUS2*. Semiquantitative plate matings indicated that overexpression of Kel1p could partially suppress the deletion (Figure 2D). If Kel1p acted solely in a parallel pathway, then we would expect that overexpression would suppress all *fus2* mutations by the same additive amount. However, in quantitative matings, Kel1p suppressed the C-terminal mutations to a much higher degree than *fus2*Δ (Figure 2E). We conclude that Kel1p overexpression partially bypasses the need for Fus2p. However, because the magnitude of Kel1p suppression was affected by the specific allele of *FUS2*, we infer that suppression is largely dependent upon residual Fus2p.

Fus2p localization is regulated by autoinhibition

Because the C-terminal mutant Fus2 proteins were mislocalized, we examined the Kel1p overexpression strains to determine if suppression caused increased localization. For both Fus2p$^{1\text{-}670}$ and Fus2p^{L674A}, Kel1p overexpression increased the number of shmoos with cortically localized Fus2p (Figure 3, A and B); however, localization was not as strong as in wild-type cells.

To identify the region of Fus2p required for Kel1p-dependent localization, we examined a series of successive 10-amino acid C-terminal truncations. In an otherwise wild-type cell, two truncations, Fus2p$^{1\text{-}660}$ and Fus2p$^{1\text{-}640}$, were severely mislocalized, comparable to Fus2p$^{1\text{-}670}$. Remarkably, Fus2p$^{1\text{-}650}$ was localized to the shmoo tip in ~50% of the shmoos (Figure 3C). However, in the cells in which Fus2p$^{1\text{-}650}$ was cortically localized, it was broadly dispersed over the shmoo tip, quite different from the discrete fluorescence observed for wild-type Fus2p (Figure 3D). All of the truncations were expressed at levels comparable to the wild-type protein and are capable of binding to Rvs161p (Stein *et al.* 2015). Because truncation of the protein to residue 650 leads to increased localization, these data suggest a model wherein a C-terminal region of Fus2p auto-inhibits interaction with the cell cortex. However, further truncation to residue 640 results in loss of localization; thus we infer that, in addition to the C terminus, sequences in the region between residues 640 and 660 are required for Fus2p localization (Figure 3E).

When Kel1p was overexpressed in the Fus2p C-terminal truncations, suppression of the localization defects was observed for both Fus2p$^{1\text{-}670}$ and Fus2p$^{1\text{-}660}$. However, Kel1p overexpression did not enhance the localization of either Fus2p$^{1\text{-}650}$ or Fus2p$^{1\text{-}640}$. Therefore, the internal localization region is also required for Kel1p overexpression-dependent localization.

Comparing the primary amino acid sequence of the C terminus of Fus2p against other fungi (Figure 1B), we found several highly conserved residues near 640. Residues D639, I640, L641, and Q642 are all conserved, with D639 and I640 being the most highly conserved across species. In addition, comparison of the C terminus of Fus2p with a known Kel1p-binding partner in mitosis, Lte1p, identified a small region of partial homology (Fus2p ^{655}VRKDW^{660}), with Fus2p-R656 and W659 matching residues in Lte1p (^{153}LKKNW^{157}). To determine if these residues were necessary for localization, we mutated each one. None of the mutations affected protein expression. D639A and I640A abolished Fus2p localization, consistent with these residues being invariant. L641A and Q642A localization was comparable to wild type. Mutations in the two residues that matched Lte1p, R656A and W659A, showed an intermediate phenotype (Figure 3F). The effects of the point mutations further indicate that residues 640–660 are important for Fus2p localization.

Kel1p plays a role in localization of Fus2p

Previous evidence showed that there are two redundant pathways for Fus2p retention at the shmoo tip. One pathway relies on Fus1p, a pheromone-induced transmembrane protein that is localized to the shmoo tip and required for cell fusion (McCaffrey *et al.* 1987; Trueheart *et al.* 1987; Trueheart and Fink 1989). The other pathway is dependent on polymerized actin (Paterson *et al.* 2008). Fus2p localization is not greatly affected either by deletion of *FUS1* or by treatment with latrunculin A to depolymerize actin. However, Fus2p is not retained at the shmoo tip when both conditions are applied (Paterson *et al.* 2008; Figure 4A). Nevertheless, point mutations in either of two regions of Fus2p (639–660 and 670–677) cause complete mislocalization. Given the redundancy of the *FUS1*- and actin-dependent pathways, these mutations must affect both pathways simultaneously.

To identify the regions of Fus2p required for each pathway, we investigated how mutations in the C terminus were affected by deletion of *FUS1* or treatment with latrunculin A. We reasoned that if one of the two pathways was specifically affected by a *fus2* mutation, then localization of the mutant protein would be significantly affected only by conditions that compromise the sole remaining pathway. In contrast, conditions that compromise the already affected pathway would have no further effect. The extreme mislocalization of Fus2p$^{1\text{-}670}$ implies that the protein cannot be localized by either pathway; as expected we found that neither deletion of *FUS1* nor treatment with latrunculin A significantly changed the Fus2p$^{1\text{-}670}$ phenotype (Figure 4A). Unlike Fus2p$^{1\text{-}670}$, Fus2p$^{1\text{-}650}$ was localized in approximately half of the cells in the population. This mutant was not affected by latrunculin A, but was completely delocalized in a *fus1*Δ mutant. We conclude that Fus2p$^{1\text{-}650}$ is localized only by the Fus1p pathway, albeit less well than the wild-type protein.

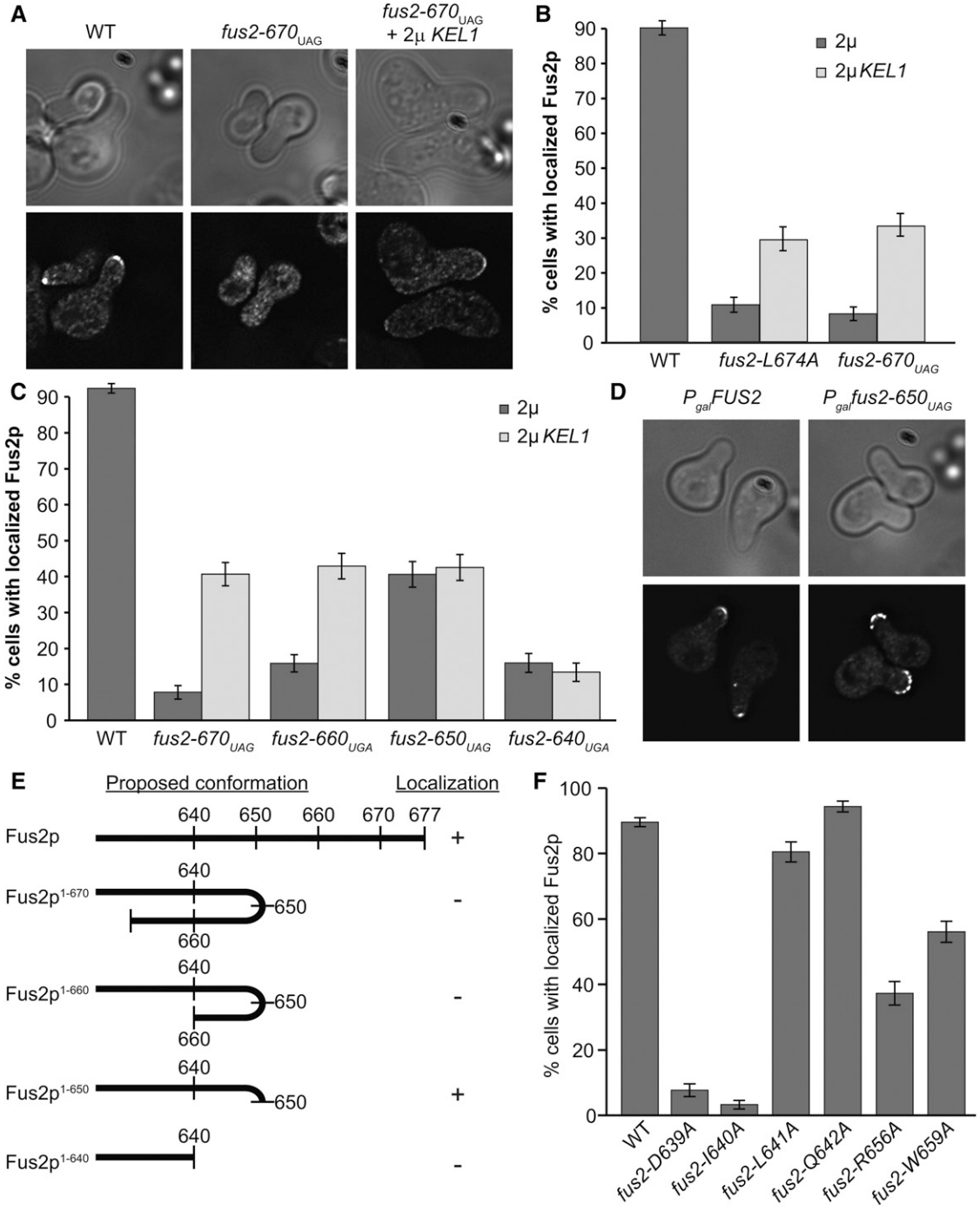

Figure 3 High-copy *KEL1* can localize certain Fus2p C-terminal mutations. (A and B) Fus2p$^{1\text{-}670}$ is localized in some cells containing high-copy *KEL1*. (A) Strains from Figure 2A were imaged after incubation with pheromone for 1.5 hr. (B) Quantification of Fus2p localization in either *fus2-L674A* or *fus2-670$_{UAG}$*. $n \geq 200$ shmoos imaged in three independent experiments. (C and D) Fus2p C-terminal truncations show differential localization phenotypes. (C) Residues 640–660 of Fus2p are important for localization as well as *KEL1* suppression. The *fus2*Δ strains (MY10904) containing WT *FUS2* (pMR5482), *fus2-670$_{UAG}$* (pMR6775), *fus2-660$_{UGA}$* (pMR6852), *fus2-650$_{UAG}$* (pMR6853), or *fus2-640$_{UGA}$* (pMR6854), all tagged internally with GFP, were imaged after incubation with pheromone for 1.5 hr. The number of shmoos with localized Fus2p was quantified for both wild-type and *KEL1* overexpression strains containing pMR6441. $n \geq 180$ shmoos imaged in three independent experiments. (D) Fus2p$^{1\text{-}650}$ is more broadly dispersed over the shmoo tip. Representative shmoos from strains containing either *FUS2* (pMR5469) or *fus2-650$_{UAG}$* (pMR6499) under the control of the Gal1 promoter. (E) Model for auto-inhibition in Fus2p C-terminal truncations. (F) Mutations in conserved residues between Fus2p 640 and 660 show differential localization phenotypes. *fus2*Δ strains (MY10904) containing *FUS2* (pMR5482), *fus2-D639A* (pMR6824), *fus2-I640A* (pMR6825), *fus2-L641A* (pMR6826), *fus2-Q642A* (pMR6827), *fus2-R656A* (pMR6828), and *W659A* (pMR6851) strains were imaged after incubation with pheromone for 1.5 hr. $n \geq 160$ shmoos imaged in three or more independent experiments.

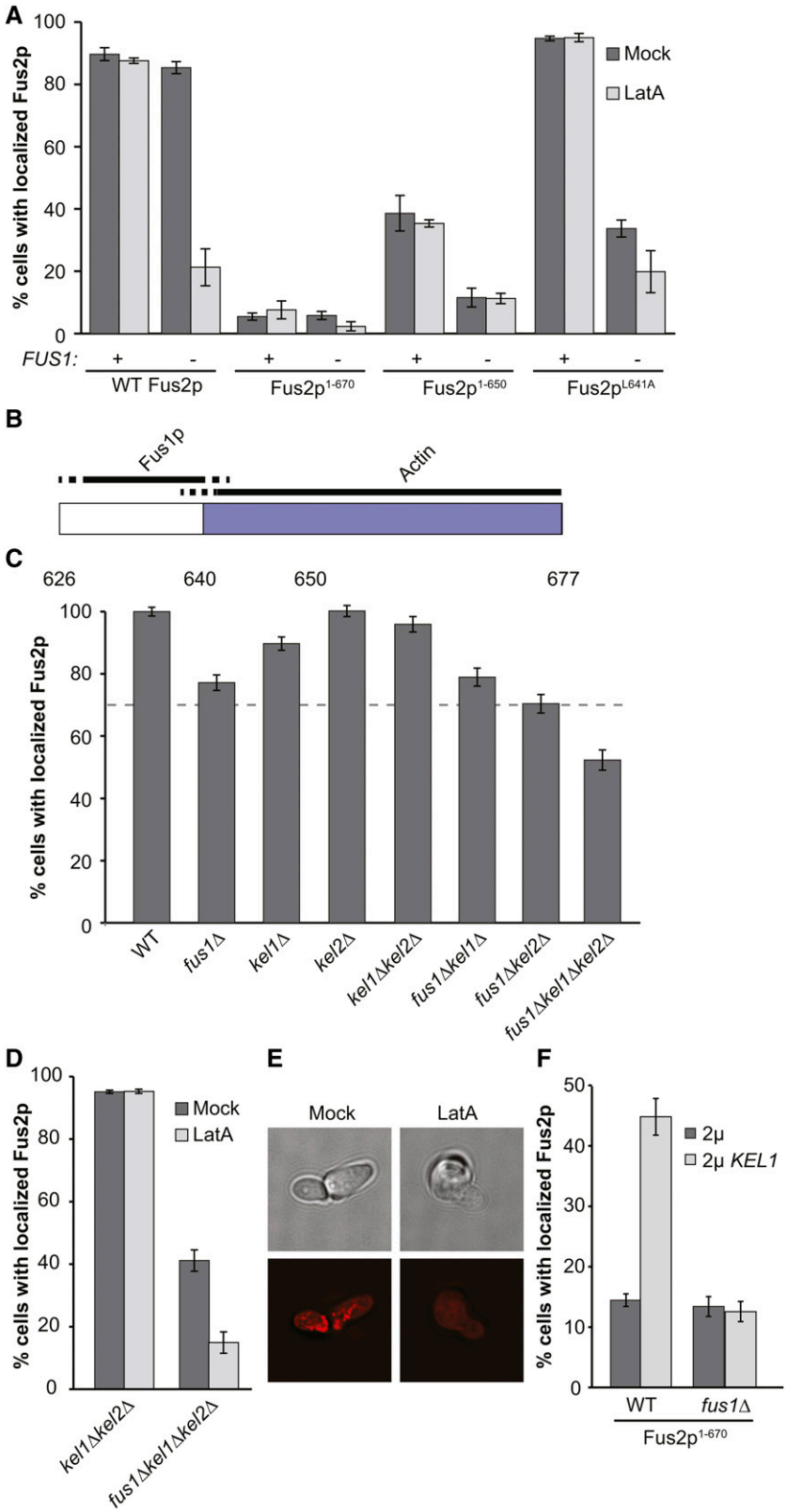

Figure 4 Fus2p is retained at the shmoo tip via Fus1p- and actin-dependent pathways. (A) The actin-dependent retention pathway acts through the C terminus of Fus2p. Shmoos containing plasmids with *FUS2* (pMR5482), *fus2-670$_{UAG}$* (pMR6775), *fus2-650$_{UAG}$* (pMR6499), or *fus2-L641A* (pMR6826) were imaged in a *fus1*Δ*fus2*Δ strain (MY10935) or in a *fus2*Δ strain (MY10904) after treatment with LatA for 5 min. Control shmoos were mock treated with DMSO. $n \geq 150$ shmoos imaged in three independent experiments. (B) Model of where the Fus1p-dependent pathway and the actin-dependent pathway act on the C terminus of Fus2p. Blue shading represents the C-terminal domain required for localization. (C) Kel1p and Kel2p play redundant roles in Fus2p localization. A plasmid containing wild-type Fus2p-GFP (pMR5482) was transformed into strains containing a *fus2*Δ (MY10904, "WT") as well as *fus1*Δ (MY10935), *kel1*Δ (MY13764), *kel2*Δ (MY13965), *fus1*Δ*kel1*Δ (MY13916), *fus1*Δ*kel2*Δ (MY14545) *kel1*Δ*kel2*Δ (MY14200), or *fus1*Δ*kel1*Δ*kel2*Δ (MY14007). Strains were imaged after treatment with pheromone for 1.5 hr. $n \geq 150$ shmoos imaged in three or more independent experiments. (D and E) Kel1p and Kel2p act through the actin-dependent pathway. (D) Fus2p localization was assessed in *kel1*Δ*kel2*Δ (MY14200) and *fus1*Δ*kel1*Δ*kel2*Δ (MY14339) strains containing pMR5482 and treated with latrunculin A. (E) Actin polymerization was assessed in *fus1*Δ*kel1*Δ*kel2*Δ via Texas Red-X Phalloidin staining after either mock or latrunculin A treatment. (F) High copy suppression of Fus2p$^{1-670}$ localization defect by Kel1p is dependent on Fus1p. *fus2*Δ (MY10904) and *fus1*Δ*fus2*Δ strains (MY10935) containing *fus2-670$_{UAG}$* (pMR6775) were transformed with either high-copy *KEL1* (pMR6441) or an empty 2μ plasmid (pRS425). The number of shmoos with localized Fus2p was quantified as before. n> 240 shmoos imaged in 3 independent experiments.

Hence, truncation of the C-terminal 27 residues mainly affects localization by the actin-dependent pathway. The third mutation, Fus2p^{L641A}, is in the conserved internal motif. This protein is indistinguishable from the wild-type protein in its localization phenotype. However, like Fus2p$^{1-650}$, there is a drastic decrease in localization when the allele is combined with *fus1*Δ, but not when the cells are treated with latrunculin A (Figure 4A). We conclude that the L641A mutation also

specifically affects the actin-dependent pathway. We interpret these data to mean that the actin-dependent pathway acts via the C terminus of Fus2p, dependent on residues 640–677. Because Fus2p$^{1\text{-}650}$ is solely dependent on Fus1p, the Fus1p-dependent pathway must act through sequences that are more internal (Figure 4B). Furthermore, because truncation of the C terminus blocks localization through both pathways, the proposed auto-inhibition must interfere with internal Fus1p-dependent localization sequences.

Because Kel1p has been implicated as an actin-binding protein (Gould *et al.* 2014), we hypothesized that it might be responsible for the actin-dependent retention pathway. To determine whether Kel1p is required for Fus2p localization, we used a *fus1*Δ background to eliminate the pathway redundancy. Because Kel1p has a homolog that may have partially redundant functions, we also examined the effect of *KEL2* deletion mutations. None of the single gene deletions caused a large decrease in Fus2p localization (Figure 4C). The same was true for double deletion mutants, whose defect was not more severe than expected from the single deletions. However, in the *fus1Δkel1Δkel2Δ* strain, only ~50% of the cells had cortically localized Fus2p, significantly worse than the 69% localization expected from combining the single mutations (P-value = 2.3×10^{-11}) (Figure 4C). Because localization was not abolished in this strain, we conclude that Kel1p and Kel2p play redundant roles in the localization of Fus2p, and that localization is largely dependent on another unidentified protein.

To determine if Kel1p and Kel2p act through the actin-dependent pathway, we analyzed localization of wild-type Fus2p in *kel1Δkel2Δ* and *fus1Δkel1Δkel2Δ* shmoos treated with latrunculin A. As before, combining *fus1Δ* with *kel1Δkel2Δ* caused a drastic decrease in Fus2p retention in the mock-treated cells (Figure 4D), showing that the actin-dependent pathway is compromised in the double mutant. Staining with Texas Red-X Phalloidin confirmed that the triple mutant does not have defects in actin polymerization (Figure 4E). In contrast, latrunculin A alone had no detectable effect on Fus2p localization in the *kel1Δkel2Δ* cells, indicating that the Fus1p-dependent pathway is fully intact in these mutants. However, latrunculin A abolished the residual localization of Fus2p in the *fus1Δkel1Δkel2Δ* mutant (Figure 4D), indicating that the actin-based pathway is still partially functional in the triple mutant. We conclude that Kel1p and Kel2p act through the actin-based pathway.

The results shown in Figure 4, A and B suggest that while Fus2p$^{1\text{-}670}$ cannot be localized by either the Fus1p- or actin-based pathway, it should retain the domain that Fus1p normally acts upon. Therefore, we wanted to determine whether localization via overexpression of Kel1p remains dependent on Fus1p or bypasses the pathway. Accordingly, we analyzed Fus2p$^{1\text{-}670}$ localization in either a wild-type or *fus1*Δ background. As before, deletion of *FUS1* had no effect on Fus2p$^{1\text{-}670}$ localization in the wild-type strain. However, deletion of *FUS1* abolished suppression by Kel1p overexpression (Figure 4F). Therefore suppression requires Fus1p, and does not bypass the normal retention pathway. Moreover, the Fus2p C-terminal truncation retains the internal sequences that mediate Fus1p-dependent localization.

Kel1p plays a role in the cell fusion pathway

Because Kel1p plays only a minor role in Fus2p localization, we next investigated suppression of cell fusion. All of the C-terminal truncations caused severe mating defects comparable to *fus2-670$_{UAG}$* (Figure 5A). Overexpression of Kel1p suppressed the *fus2-660$_{UGA}$* and *fus2-640$_{UGA}$* mutations, but only slightly increased the mating efficiency of the *fus2-650$_{UAG}$* mutation (Figure 5B). Surprisingly, the mating efficiency of the *fus2-650$_{UAG}$* mutant was not significantly enhanced by Kel1p overexpression (P-value = 0.1), similar to the efficiency of the suppressed *fus2*Δ mutant (P-value = 0.3, Figure 5A). This was true even though Fus2p$^{1\text{-}650}$ localized to the shmoo tip as well as or better than any of the other mutants. These data suggest that the mutant Fus2p$^{1\text{-}650}$ may actually interfere with cell fusion. If so, we predict that *fus2-650$_{UAG}$* would be dominant.

To test dominance, we examined mating efficiency in a strain that contained a wild-type copy of *FUS2* on the chromosome and a copy of *fus2-650$_{UAG}$* on a centromeric plasmid. Note that the mating efficiency of the wild-type strain to a *fus1Δfus2Δ* partner was increased when a second copy of *FUS2* was present, indicating that Fus2p function is limiting during these mating conditions. The *fus2-670$_{UAG}$* plasmid was essentially neutral, with no increase in mating efficiency. In contrast, the *fus2-650$_{UAG}$* plasmid caused decreased mating compared to wild type or *fus2-670$_{UAG}$* (Figure 5B); therefore we conclude that *fus2-650$_{UAG}$* is semidominant. Finally, Kel1p overexpression significantly suppressed the *fus2-640$_{UGA}$* mutation (Figure 5A), even though it did not enhance the localization of Fus2p$^{1\text{-}640}$. Taken together, these data lead us to conclude that overexpression of Kel1p suppresses by at least two mechanisms: (1) bypassing the need for Fus2p and (2) enhancing the localization and/or activity of Fus2p.

It was previously shown that deletion of either *KEL1* or its homolog *KEL2* caused only a small increase in the number of unfused zygotes when mated against a wild-type partner (Philips and Herskowitz 1998). We found that loss of either *KEL1* or *KEL2* resulted in a significant decrease in cell fusion efficiency when mated to a *fus1Δfus2Δ* mating partner. The defect was not exacerbated in the double mutant (Figure 5C), suggesting that the proteins act together during cell fusion, consistent with them acting as heterodimers (Philips and Herskowitz 1998).

Kel1p and Fus2p physically interact in pheromone-induced cells

The suppression of Fus2p localization defects by Kel1p suggests that these two proteins might physically interact. We tested this hypothesis by performing co-immunoprecipitations in pheromone-induced cells. Kel1p was C-terminally tagged with a 3× HA epitope at the *KEL1* locus. The tagged protein was also cloned onto a 2μ vector because suppression is only observed

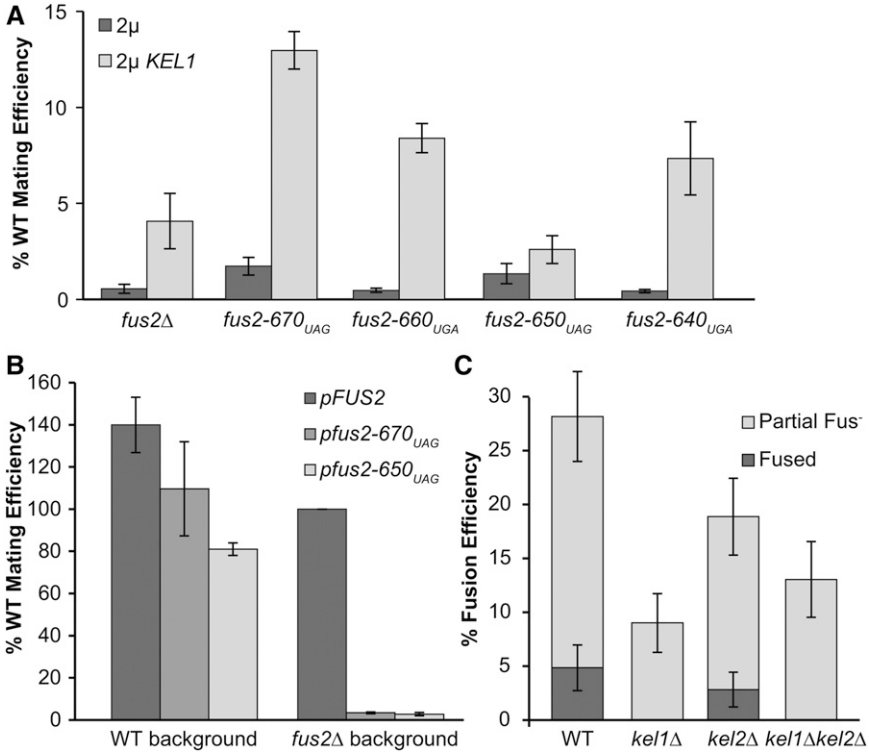

Figure 5 High-copy *KEL1* differentially suppresses the mating phenotype of mutations in *FUS2*. (A) High-copy *KEL1* suppresses Fus2p$^{1\text{-}640}$ and Fus2p$^{1\text{-}660}$. The same strains as in Figure 3C were mated to a *fus1*Δ*fus2*Δ (JY429) for 4 hr at 30° and suppression was assessed via diploid formation. (B) Fus2p$^{1\text{-}650}$ is semidominant. Plasmids containing *FUS2* (pMR5482), *fus2-670*$_{UAG}$ (pMR6775), or *fus2-650*$_{UAG}$ (pMR6853) were transformed into either a *FUS2* (BY4741) or *fus2*Δ (MY10904) background. These strains were mated to a *fus1*Δ*fus2*Δ (JY429) for 4 hr at 30° and suppression was assessed via diploid formation. (C) Kel1p and Kel2p act together during cell fusion. Strains containing deletions in *KEL1* (MY13675), *KEL2* (MY13676), or both (MY13765) were mated to a *fus1*Δ*fus2*Δ (JY429) for 2.5 hr at 30°, resuspended in TAF buffer, and incubated with FM4-64 to stain the plasma membrane. Percentage of fully fused and partially fused zygotes observed for each genotype is shown. $n \geq 92$ zygotes imaged in three independent experiments.

with Kel1p overexpression. Both constructs were functional for mating and suppression. Fus2p was internally tagged with GFP and fully functional (Paterson *et al.* 2008). Wild-type Fus2p coprecipitated with both single-copy and high-copy Kel1p (Figure 6A), proportional to the amount of Kel1p present in the cell. These results support the hypothesis that Kel1p and Fus2p interact, although the interaction may be indirect.

We next tested the interaction of Kel1p with the Fus2p C-terminal truncations. Surprisingly, Kel1p interacted with all of the C-terminal truncations (Figure 6B). Kel1p also interacted with both a more extensive C-terminal truncation (Fus2p$^{1\text{-}580}$) and an N-terminal truncation (Fus2p$^{105\text{-}677}$, Figure 6C), although deletion of the C-terminal residues partially reduced binding. These data defined the region capable of binding to Kel1p to be between residues 105 and 580 on Fus2p. We next tested three fragments, Fus2p$^{\Delta 105\text{-}415}$, Fus2p$^{1\text{-}415}$, and Fus2p$^{1\text{-}104}$. Remarkably, the only fragment not able to interact with Kel1p was Fus2p$^{1\text{-}104}$ (Figure 6C). Thus there are two regions of Fus2p that interact with Kel1p, one between residues 104 and 415, corresponding to the DBH domain, and one between residues 415 and 677, containing the RBD (Figure 6D). However, interaction with the C-terminal region appears to be significantly more efficient than via the DBH domain.

Kel1p functions with Cdc42p to mediate cell fusion

Although Kel1p plays a role in localizing Fus2p, the ability of Kel1p overexpression to partially suppress a *fus2*Δ suggests that Kel1p must also have a Fus2p-independent function in cell fusion. To examine this further, we determined if deletions of both *FUS2* and *KEL1* caused a synthetic mating defect. When the efficiency of mating to a *fus2*Δ mutant was measured, we found that the mating efficiency of the double mutant (9 ± 3%) was not significantly different (*P*-value = 0.32) from the expectation based on a multiplicative model (10%, Figure 7A), suggesting that Kel1p and Fus2p may have some independent functions for mating.

Fus2p interacts with GTP-bound Cdc42p and the interaction is required for fusion but not for Fus2p localization (Ydenberg *et al.* 2012). To determine if the Fus2p-independent function of Kel1p requires Cdc42p, we examined suppression of a mutant of Cdc42p (*cdc42-138)* that abolishes interaction with Fus2p (Ydenberg *et al.* 2012). Kel1p overexpression suppressed *cdc42-138*, bringing the mating efficiency to wild-type levels when mated to a *fus1*Δ*fus2*Δ strain (Figure 7B). To determine if suppression is dependent on Fus2p, we assessed suppression in a *cdc42-138 fus2*Δ strain. Overexpression of Kel1p increased the mating efficiency of this strain very slightly, not nearly to the level of *cdc42-138* alone (Figure 7B); therefore suppression of *cdc42-138* is Fus2p dependent. Because overexpression of Kel1p suppresses the defect associated with a defective Cdc42p–Fus2p interaction, without bypassing Fus2p, we infer that Kel1p must facilitate their interaction. One way this may occur would be if the three proteins function in a ternary complex.

We next investigated the combination of *cdc42-138* and *kel1*Δ. The double mutant exhibited significant (*P*-value = 0.03) negative epistasis (Figure 7C), based on an expected mating efficiency of 8.4% for independent pathways and an observed mating efficiency of 2 ± 0.2%. The negative interaction between these two mutations suggests that Kel1p is required for the residual cell fusion activity in the *cdc42-138* mutant.

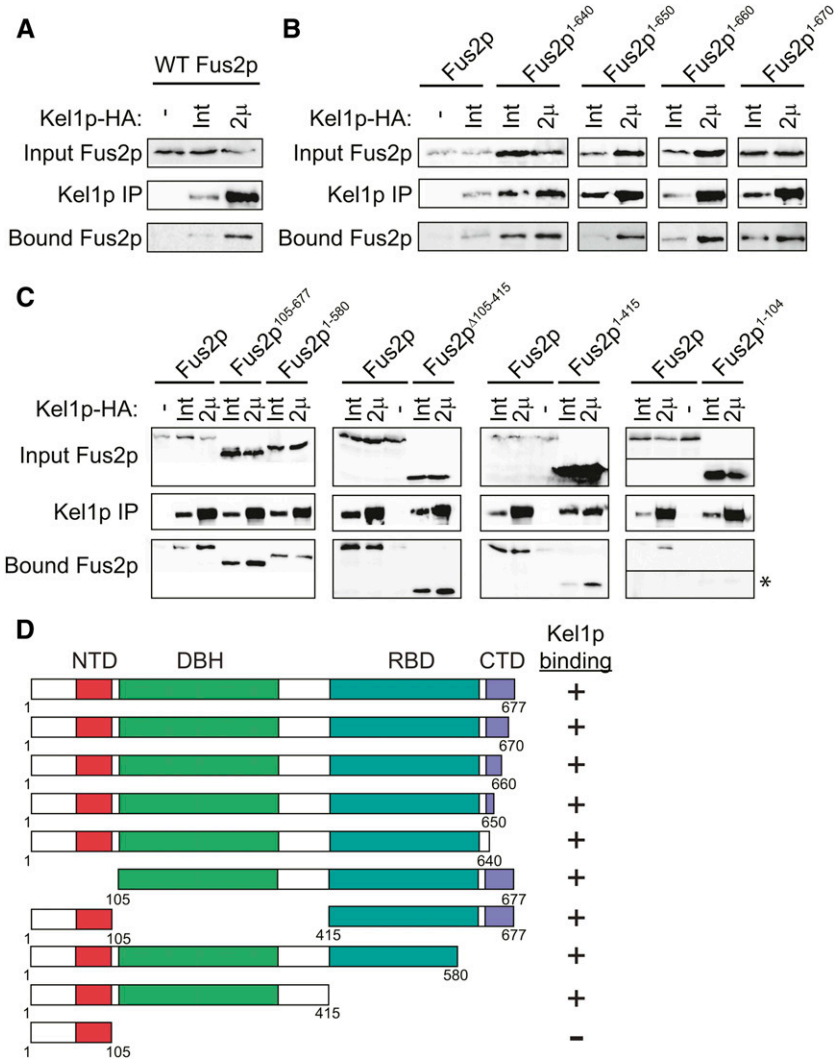

Figure 6 Fus2p and Kel1p interact in pheromone-induced cells. (A) Wild-type Fus2p interacts with Kel1p. *KEL1* tagged with 3× HA was either integrated (Int) at the *KEL1* locus (MY15063) or cloned on to a 2μ vector (pMR6953). These constructs along with untagged *KEL1* (−) were pulled down with anti-HA magnetic beads. Interaction with GFP-tagged Fus2p (pMR5482) was assessed via Western blot with anti-GFP antibodies. (B) All Fus2p C-terminal truncations interact with Kel1p. Co-immunoprecipitations were performed as in A with strains containing Fus2p$^{1\text{-}640}$ (pMR6854), Fus2p$^{1\text{-}650}$ (pMR6853), Fus2p$^{1\text{-}660}$ (pMR6854), or Fus2p$^{1\text{-}670}$ (pMR6775). (C and D) Kel1p has two binding sites on Fus2p. (C) Interaction with Kel1p was tested with strains containing Fus2p$^{105\text{-}677}$ (pMR5784), Fus2p$^{1\text{-}580}$ (pMR5886), Fus2p$^{\Delta 105\text{-}415}$ (pMR5883), Fus2p$^{1\text{-}415}$ (pMR7008), and (Fus2p$^{1\text{-}104}$ (pMR5774). Because the Fus2p$^{1\text{-}104}$ fragment is much smaller than wild-type Fus2p (38 kDa *vs.* 102 kDa), we show the input Fus2p and bound Fus2p panels with the center removed, denoted by a black line. The asterisk denotes where Fus2p$^{1\text{-}104}$ would run if it bound Kel1p-HA. (D) Map of all Fus2p fragments tested summarizing the results of the binding experiments.

When the interaction between Cdc42p and Fus2p was mapped, Cdc42p was found to strongly interact with the Dbl-homology domain in the N terminus of Fus2p and weakly interact with a region in the C terminus (Ydenberg *et al.* 2012). Given that both Cdc42p and Kel1p are able to bind to two domains of Fus2p, we wanted to determine if the Kel1p interaction with either the N or C terminus was dependent upon the Cdc42p–Fus2p interaction. Therefore, we performed coprecipitations of Kel1p with full-length Fus2p as well as the N- (Fus2p$^{1\text{-}415}$) and C-terminal fragments (Fus2p$^{415\text{-}677}$) in either a wild-type *CDC42* or *cdc42-138* background. The interaction between full-length Fus2p and Kel1p was not significantly (*P*-value = 0.7) altered in the *cdc42-138* background (Figure 7D). However, binding of both fragments of Fus2p to Kel1p was strongly affected in a *cdc42-138* background (Figure 7D). Therefore, we conclude that the interaction between Kel1p and both of the Fus2p fragments is dependent upon Cdc42p–Fus2p binding. We hypothesize that the three proteins form a complex with Cdc42p contributing to the stability of binding to each individual domain.

Discussion

Kel1p has multiple functions in cell fusion

Here we show that Kel1p has multiple functions in the cell fusion pathway. First, Kel1p has a role in enhancing the localization of Fus2p. Kel1p and Kel2p play redundant roles in localizing wild-type Fus2p in mating cells (Figure 4) and overexpression of Kel1p suppresses the mislocalization of C-terminal Fus2p mutants. Kel1p overexpression had no effect on the localization of truncated proteins lacking the 37 C-terminal residues, suggesting that Kel1p-mediated Fus2p localization requires sequences near the C terminus of Fus2p (Figure 2 and Figure 3). However, Kel1p is neither essential nor sufficient for Fus2p localization. The complexity of Fus2p localization may be understood by considering that successful cell wall breakdown is essential for sexual conjugation, but misplaced or ill-timed breakdown would jeopardize viability.

The second function of Kel1p is to promote cell fusion through Fus2p and Cdc42p. It is thought that Fus2p localizes GTP-bound Cdc42p to the zone of cell fusion, where it

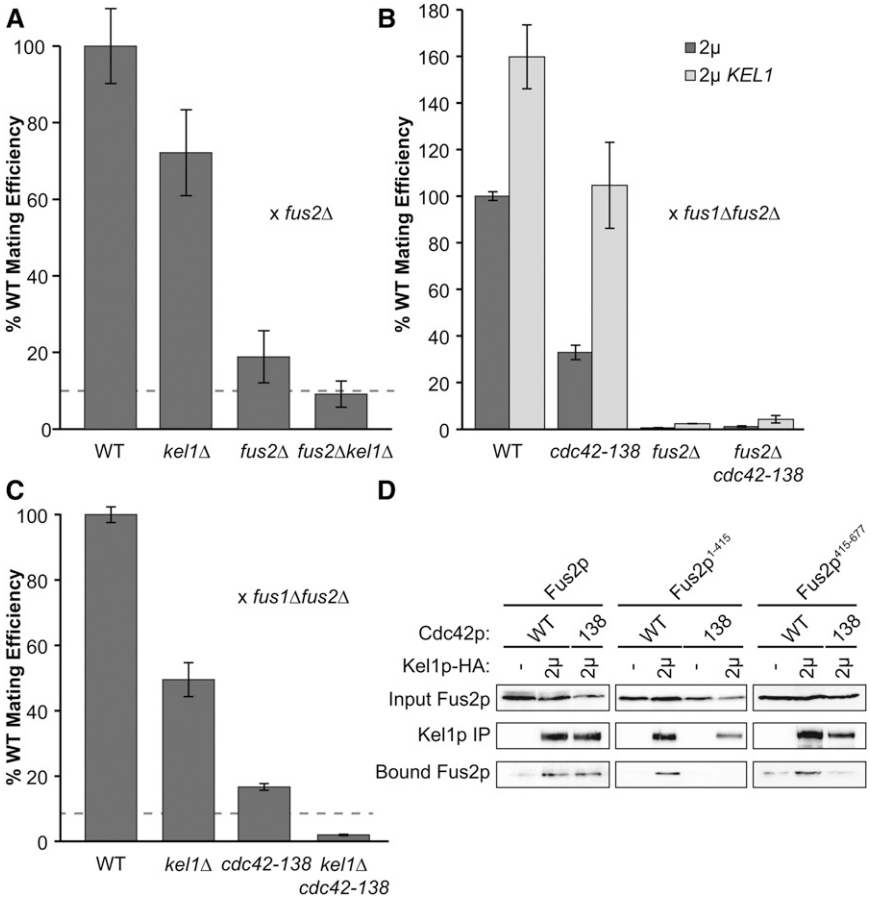

Figure 7 Kel1p plays a Fus2p-independent Cdc42p-dependent role in mating. (A) Deletions in *fus2* and *kel1* show a synthetic mating phenotype. Wild-type (BY4741), *fus2*Δ (MY10904), *kel1*Δ (MY13675), and *fus2*Δ*kel1*Δ (MY13764) strains were mated against a *fus2*Δ (JY428) for 3 hr at 30°. Mating efficiency was assessed via diploid formation. Dotted lines represent the expectation for the double deletion based on the multiplicative model for single deletions. (B) High-copy *KEL1* suppresses the mating defect of *cdc42-138* in a *FUS2*-dependent manner. Strains containing a *fus2*Δ as well as the *cdc42-138* mutation integrated at the *CDC42* locus (MY15474) or wild-type *CDC42* (MY15471) were transformed with wild-type *FUS2* (pMR5482) and either high-copy *KEL1* (pMR6441) or an empty vector (pRS425). *fus2*Δ strains were transformed with an empty vector (pRS425) instead of pMR5482. All strains were mated against a *fus1*Δ*fus2*Δ (JY429) for 2.5 hr at 30° and mating efficiency was assessed via diploid formation. (C) Deletion of *KEL1* shows negative epistasis when combined with *cdc42-138*. Wild-type (BY4741), *kel1*Δ (MY13675), *cdc42-138* (MY15473) and *kel1*Δ*cdc42-138* (MY15475) strains were mated against a *fus1*Δ*fus2*Δ strain (JY429) for 2.5 hr at 30°. Mating efficiency was assessed via diploid formation. Dotted lines represent the expectation for the double deletion based on the multiplicative model for single deletions. (D) Fus2p$^{1-415}$ and Fus2p$^{415-677}$ are dependent upon *CDC42* for binding to Kel1p. *CDC42 fus2*Δ (MY15471) or *cdc42-138 fus2*Δ (MY15474) strains were transformed with a plasmid containing either full-length *FUS2* (pMR5469) or fragments containing residues 1–415 (pMR7008) or 415–677 (pMR5884) tagged with GFP. These strains were also transformed with either high-copy *KEL1-3xHA* (pMR6953) or an empty vector (pRS423). Co-immunoprecipitation experiments were performed as in Figure 6.

activates fusion of vesicles with the plasma membrane to release hydrolases that break down the cell wall. Deletion of *KEL1* showed a strong synthetic mating phenotype with a point mutation in *CDC42* that abolishes interaction with Fus2p (*cdc42-138*) (Figure 7). One interpretation of this negative epistasis is that Kel1p and Cdc42p must act together to mediate cell fusion. The finding that overexpression of Kel1p fully suppressed the mating defect of *cdc42-138*, but remained dependent upon Fus2p, supports the view that Kel1p's function in mating involves Cdc42p (Figure 7). Overexpression suppression of *cdc42-138* might stabilize the defective Cdc42–Fus2p interaction or position the two proteins in close enough proximity to function.

Kel1p's third function is through a Fus2p-independent, but presumably Cdc42p-dependent pathway. The ability of Kel1p to weakly suppress a full deletion of *FUS2* implies that Kel1p can partially bypass the need for Fus2p in cell fusion (Figure 5). Kel1p is localized to the shmoo tip (Philips and Herskowitz 1998). If Kel1p binds active Cdc42p, then partial suppression of *fus2*Δ may be due to inefficient localization of Cdc42p at the shmoo tip.

Kel1p overexpression also suppresses the mating defects associated with deletion of *SPA2* and *FPS1*, as well as a hyperactive allele of *PKC1* (*PKC1-R398P*) (Philips and Herskowitz 1998). Spa2p is a component of the polarisome and is required for actin cytoskeletal organization during polarized growth. The mating defect in *spa2*Δ was hypothesized to be due to lack of vesicle clustering across the zone of cell fusion (Gammie *et al.* 1998). Fps1p is a glycerol efflux pump (Luyten *et al.* 1995), hypothesized to cause a fusion defect due to the lack of osmotic balance between the two mating cells (Philips and Herskowitz 1997). Pkc1p, a member of the cell wall integrity (CWI) pathway in yeast, also has roles in osmotic regulation (Davenport *et al.* 1995). Because hyperactive Pkc1p blocks fusion, it was suggested that the CWI pathway negatively regulates fusion (Philips and Herskowitz 1997). Interestingly, Spa2p also acts as a scaffold for the Mkk1p and Mpk1p CWI signaling components (Van Drogen and Peter 2002). The observation that all of these proteins are involved in the CWI pathway suggests Kel1p may be part of the mechanism by which these pathways regulate cell fusion. Deletion of *KEL1* showed synthetic mating defects with *fps1*Δ, *fus2*Δ, *fus1*Δ, and *PKC1-R398P* but not with *spa2*Δ (Philips and Herskowitz 1998), suggesting that Kel1p may function in the same pathway as Spa2p.

Kel1p has functions in both mitotic and mating cells. In mitotic cells, Kel1p localizes to the bud cortex where it interacts with Kel2p and Lte1p (Philips and Herskowitz 1998;

Seshan *et al.* 2002). Lte1p, a member of the mitotic exit network, has homology to GEFs and is asymmetrically localized to the bud cortex during S phase (Shirayama *et al.* 1994; Bardin *et al.* 2000; Pereira *et al.* 2000). Kel1p has been shown to anchor Lte1p to the bud cortex, along with other factors (Seshan *et al.* 2002). We therefore hypothesize that Kel1p may also serve as a scaffold in polarized cells for cell-fusion-specific proteins such as Fus2p and Cdc42p.

Kel1p and Kel2p contribute to the actin-dependent pathway for Fus2p localization

Previous research showed that Fus2p localization is dependent upon Fus1p and the actin cytoskeleton, acting redundantly (Paterson *et al.* 2008; Sheltzer and Rose 2009). The protein(s) involved in the actin-dependent pathway is unknown. Our data show that Kel1p and Kel2p contribute to Fus2p localization through the actin-based pathway. However, the residual localization of Fus2p in the *fus1*Δ *kel1*Δ*kel2*Δ mutant implies that localization is mediated by a third redundant protein that was not identified by our mutant screen (Figure 4).

Despite the saturation of our overexpression screen, there are many reasons why we did not find the other protein required for actin-dependent Fus2p localization. Assuming that the unknown protein binds to the last 10 amino acids of Fus2p, the point mutations may reduce binding to a level that cannot be suppressed by overexpression. Alternatively, overexpression of the Fus2p-binding protein may cause it to be mislocalized. This would decrease mating efficiency by sequestering Fus2p to ectopic sites. Finally it is possible that the localizing protein requires a limiting modification, such that overexpression does not alter the concentration of active protein able to localize Fus2p. The other protein identified in this screen, Mps1p, is a dual-specificity kinase required for spindle pole body duplication and spindle checkpoint function (Winey *et al.* 1991). While further characterization of suppression has not been carried out, we hypothesize that Mps1p may phosphorylate a protein required for localization, which would explain why we did not identify the target from the overexpression screen. Future work to identify the missing protein or proteins required for Fus2p localization is ongoing.

Kel1p interacts with two domains of Fus2p

Directly or indirectly, Kel1p interacts with at least two domains of Fus2p; one is between amino acids 104 and 415, and the other is between amino acids 415 and 677 (Figure 6). Based on the suppression data, we hypothesize that the interaction with the C terminus is required for Kel1p's function in localizing Fus2p. We do not yet know the functional significance of Kel1p's interaction with Fus2p's N terminus. However, it may be responsible for suppression of the mating defect, given that Kel1p suppresses a mutant, Fus2p$^{1\text{-}640}$, which is not localized by overexpression (Figure 3 and Figure 5).

We hypothesize that Kel1p, Fus2p, and Cdc42p form a multimeric complex in polarized cells. GTP-bound Cdc42p has been shown to strongly interact with the DBH domain of Fus2p, but also weakly interacted with the C terminus (Ydenberg *et al.* 2012). Kel1p also interacts with both of these domains (Figure 6), albeit more strongly to the C-terminal domain. Interestingly, interaction of Kel1p with both Fus2p domains was dependent upon the Fus2p–Cdc42p interaction (Figure 7). However, Cdc42p dependence was not observed for the interaction between full-length Fus2p and Kel1p. These data suggest that the Kel1p interaction with each domain of Fus2p may be of lower affinity and require stabilization by interaction with Cdc42p in a ternary complex. When both domains are present, the Kel1p–Fus2p interaction would be much stronger and independent of Cdc42p. Taken together, these data suggest that Kel1p plays a critical role in the Fus2p–Cdc42p regulation of cell fusion.

Acknowledgments

We thank members of the Rose and Gammie laboratories for helpful support and discussion. We especially thank Richard Stein for constructing the original C-terminal Fus2p mutations. We thank Danelle Devenport for helpful suggestions. This work was supported by National Institutes of Health Grants GM037739 (to M.D.R.). J.A.S. was supported by National Institutes of Health Training Grant GM007388.

Literature Cited

Adamo, J. E., J. J. Moskow, A. S. Gladfelter, D. Viterbo, D. J. Lew *et al.*, 2001 Yeast Cdc42 functions at a late step in exocytosis, specifically during polarized growth of the emerging bud. J. Cell Biol. 155: 581–592.

Adams, J., R. Kelso, and L. Cooley, 2000 The kelch repeat superfamily of proteins: propellers of cell function. Trends Cell Biol. 8924: 17–24.

Amberg, D. C., D. J. Burke, and J. N. Strathem, 2005 *Methods in Yeast Genetics: A Cold Spring Harbor Laboratory Course Manual*, Cold Spring Harbor Laboratory Press, Cold Spring Harbor, NY.

Baba, M., N. Baba, Y. Ohsumi, K. Kanaya, and M. Osumi, 1989 Three-dimensional analysis of morphogenesis induced by mating pheromone α factor in *Saccharomyces cerevisiae*. J. Cell Sci. 94(Pt 2): 207–216.

Bardin, A. J., R. Visintin, and A. Amon, 2000 A mechanism for coupling exit from mitosis to partitioning of the nucleus. Cell 102: 21–31.

Bertazzi, D. T., B. Kurtulmus, and G. Pereira, 2011 The cortical protein Lte1 promotes mitotic exit by inhibiting the spindle position checkpoint kinase Kin4. J. Cell Biol. 193: 1033–1048.

Brachmann, C. B., A. Davies, G. J. Cost, E. Caputo, J. Li *et al.*, 1998 Designer deletion strains derived from *Saccharomyces cerevisiae* S288C: a useful set of strains and plasmids for PCR-mediated gene disruption and other applications. Yeast 14: 115–132.

Brizzio, V., A. E. Gammie, and M. D. Rose, 1998 Rvs161p interacts with Fus2p to promote cell fusion in *Saccharomyces cerevisiae*. J. Cell Biol. 141: 567–584.

Broach, J. R., J. N. Strathern, and J. B. Hicks, 1979 Transformation in yeast: development of a hybrid cloning vector and isolation of the CAN1 gene. Gene 8: 121–133.

Crouzet, M., M. Urdaci, L. Dulau, and M. Aigle, 1991 Yeast mutant affected for viability upon nutrient starvation: characterization and cloning of the RVS161 gene. Yeast 7: 727–743.

Davenport, K. R., M. Sohaskey, Y. Kamada, D. E. Levin, and M. C. Gustin, 1995 An osmosensing signal transduction pathway in yeast. Hypotonic shock activates the Pkc1 protein kinase-regulated cell integrity pathway. J. Biol. Chem. 270: 30157–30161.

Friesen, H., C. Humphries, Y. Ho, O. Schub, K. Colwill *et al.*, 2006 Characterization of the yeast Amphiphysins Rvs161p and Rvs167p reveals roles for the Rvs heterodimer in vivo. Mol. Biol. Cell 17: 1306–1321.

Galbraith, A. M., and R. E. Malone, 1993 Characterization of *REC104*, a gene required for early meiotic recombination in the yeast *Saccharomyces cerevisiae*. Dev. Genet. 13: 392–402.

Gammie, A. E., V. Brizzio, and M. D. Rose, 1998 Distinct morphological phenotypes of cell fusion mutants. Mol. Biol. Cell 9: 1395–1410.

Gammie, A. E., and M. D. Rose, 2002 Assays of cell and nuclear fusion, pp. 477–498 in *Methods in Enzymology*, edited by C. Guthrie, and G. R. Fink. Academic Press, San Diego.

Gauster, M., G. Moser, K. Orendi, and B. Huppertz, 2009 Factors involved in regulating trophoblast fusion: potential role in the development of preeclampsia. Placenta 30 (Suppl A): S49–S54.

Gould, C. J., M. Chesarone-Cataldo, S. L. Alioto, B. Salin, I. Sagot *et al.*, 2014 *Saccharomyces cerevisiae* Kelch proteins and Bud14 protein form a stable 520-kDa formin regulatory complex that controls actin cable assembly and cell morphogenesis. J. Biol. Chem. 289: 18290–18301.

Grote, E., 2008 Cell fusion assays for yeast mating pairs. Methods Mol. Biol. 475: 165–196.

Heiman, M. G., and P. Walter, 2000 Prm1p, a pheromone-regulated multispanning membrane protein, facilitates plasma membrane fusion during yeast mating. J. Cell Biol. 151: 719–730.

Höfken, T., and E. Schiebel, 2002 A role for cell polarity proteins in mitotic exit. EMBO J. 21: 4851–4862.

Huppertz, B., and M. Borges, 2008 Placenta trophoblast fusion. Methods Mol. Biol. 475: 135–147.

Johnson, D. I., 1999 Cdc42: an essential Rho-type GTPase controlling eukaryotic cell polarity. Microbiol. Mol. Biol. Rev. 63: 54–105.

Kim, J., and M. D. Rose, 2012 A mechanism for the coordination of proliferation and differentiation by spatial regulation of Fus2p in budding yeast. Genes Dev. 26: 1110–1121.

Kim, J. H., P. Jin, R. Duan, and E. H. Chen, 2015 Mechanisms of myoblast fusion during muscle development. Curr. Opin. Genet. Dev. 32: 162–170.

Kozminski, K. G., A. J. Chen, A. A. Rodal, and D. G. Drubin, 2000 Functions and functional domains of the GTPase Cdc42p. Mol. Biol. Cell 11: 339–354.

Luyten, K., J. Albertyn, W. F. Skibbe, B. A. Prior, J. Ramos *et al.*, 1995 Fps1, a yeast member of the MIP family of channel proteins, is a facilitator for glycerol uptake and efflux and is inactive under osmotic stress. EMBO J. 14: 1360–1371.

McCaffrey, G., F. J. Clay, K. Kelsay, and G. F. Sprague, 1987 Identification and regulation of a gene required for cell fusion during mating of the yeast Saccharomyces cerevisiae. Mol. Cell. Biol. 7: 2680–2690.

Merlini, L., O. Dudin, and S. G. Martin, 2013 Mate and fuse: how yeast cells do it. Open Biol. 3: 130008.

Nelson, B., A. B. Parsons, M. Evangelista, K. Schaefer, K. Kennedy *et al.*, 2004 Fus1p interacts with components of the Hog1p mitogen-activated protein kinase and Cdc42p morphogenesis signaling pathways to control cell fusion during yeast mating. Genetics 166: 67–77.

Ohashi, A., J. Gibson, I. Gregor, and G. Schatz, 1982 Import of proteins into mitochondria. The precursor of cytochrome c1 is processed in two steps, one of them heme-dependent. J. Biol. Chem. 257: 13042–13047.

Paterson, J. M., C. A. Ydenberg, and M. D. Rose, 2008 Dynamic localization of yeast Fus2p to an expanding ring at the cell fusion junction during mating. J. Cell Biol. 181: 697–709.

Pereira, G., T. Höfken, J. Grindlay, C. Manson, and E. Schiebel, 2000 The Bub2p spindle checkpoint links nuclear migration with mitotic exit. Mol. Cell 6: 1–10.

Philips, J., and I. Herskowitz, 1997 Osmotic balance regulates cell fusion during mating in *Saccharmyces cerevisiae*. J. Cell Biol. 138: 961–974.

Philips, J., and I. Herskowitz, 1998 Identification of Kel1p, a Kelch domain-containing protein involved in cell fusion and morphology in Saccharomyces cerevisiae. J. Cell Biol. 143: 375–389.

Richman, T. J., M. M. Sawyer, and D. I. Johnson, 1999 The Cdc42p GTPase is involved in a G_2/M morphogenetic checkpoint regulating the apical-isotropic switch and nuclear division in yeast. J. Biol. Chem. 274: 16861–16870.

Seshan, A., A. J. Bardin, and A. Amon, 2002 Control of Lte1 localization by cell polarity determinants and Cdc14. Curr. Biol. 12: 2098–2110.

Sheltzer, J. M., and M. D. Rose, 2009 The class V myosin Myo2p is required for Fus2p transport and actin polarization during the yeast mating response. Mol. Biol. Cell 20: 2909–2919.

Shirayama, M., Y. Matsui, K. Tanaka, and A. Toh-e, 1994 Isolation of a CDC25 family gene, MSI2/LTE1, as a multicopy suppressor of ira1. Yeast 10: 451–461.

Sikorski, R. S., and P. Hieter, 1989 A system of shuttle vectors and yeast host strains designed for efficient manipulation of DNA in Saccharomyces cerevisiae. Genetics 122: 19–27.

Stein, R. A., J. A. Smith, and M. D. Rose, 2015 An amphiphysin-like domain in Fus2p is required for Rvs161p interaction and cortical localization. G3 (Bethesda) 6: 337–349.

Trueheart, J., and G. R. Fink, 1989 The yeast cell fusion protein FUS1 is O-glycosylated and spans the plasma membrane. Proc. Natl. Acad. Sci. USA 86: 9916–9920.

Trueheart, J., J. D. Boeke, and G. R. Fink, 1987 Two genes required for cell fusion during yeast conjugation: evidence for a pheromone-induced surface protein. Mol. Cell. Biol. 7: 2316–2328.

Van Drogen, F., and M. Peter, 2002 Spa2p functions as a scaffold-like protein to recruit the Mpk1p MAP kinase module to sites of polarized growth. Curr. Biol. 12: 1698–1703.

Wassarman, P. M., and E. S. Litscher, 2008 Mammalian fertilization is dependent on multiple membrane fusion events. Methods Mol. Biol. 475: 99–113.

Winey, M., and B. J. Huneycutt, 2002 Centrosomes and checkpoints: the MPS1 family of kinases. Oncogene 21: 6161–6169.

Winey, M., L. Goetsch, P. Baum, and B. Byers, 1991 *MPS1* and *MPS2*: novel yeast genes defining distinct steps of spindle pole body duplication. J. Cell Biol. 114: 745–754.

Ydenberg, C. A., and M. D. Rose, 2008 Yeast mating: a model system for studying cell and nuclear fusion. Methods Mol. Biol. 475: 3–20.

Ydenberg, C. A., and M. D. Rose, 2009 Antagonistic regulation of Fus2p nuclear localization by pheromone signaling and the cell cycle. J. Cell Biol. 184: 409–422.

Ydenberg, C. A., R. A. Stein, and M. D. Rose, 2012 Cdc42p and Fus2p act together late in yeast cell fusion. Mol. Biol. Cell 23: 1208–1218.

Communicating editor: O. Cohen-Fix